

# Amino acids as chelating ligands for platinum: enhanced stability in aqueous environment promoted by biocompatible molecules

Andrea Cucchiaro<sup>1</sup>, Amelie Scherfler<sup>1</sup>, Davide Corinti<sup>2</sup>, Giel Berden<sup>3</sup>, Jos Oomens<sup>3</sup>, Klaus Wurst<sup>4</sup>, Ronald Gust<sup>1#</sup>, Maria Elisa Crestoni<sup>2</sup>, Brigitte Kircher<sup>5,6</sup>, Monika Cziferszky<sup>1,\*</sup>

1. Institute of Pharmacy, Pharmaceutical Chemistry, Center for Molecular Biosciences Innsbruck, University of Innsbruck, Innrain 80-82, A-6020 Innsbruck, Austria
2. Dipartimento di Chimica e Tecnologie del Farmaco, Università di Roma "La Sapienza", P. le A. Moro 5, I-00185 Roma, Italy
3. Radboud University, Institute for Molecules and Materials, FELIX Laboratory, Toernooiveld 7, 6525ED Nijmegen, the Netherlands
4. Institute of General, Inorganic and Theoretical Chemistry, University of Innsbruck, CCB—Centrum for Chemistry and Biomedicine, Innrain 80-82, 6020 Innsbruck, Austria
5. Tyrolean Cancer Research Institute, Innrain 66, 6020 Innsbruck, Austria
6. Immunobiology and Stem Cell Laboratory, Department of Internal Medicine V (Hematology and Oncology), Innsbruck Medical University, Anichstraße 35, 6020 Innsbruck, Austria

Correspondence: [monika.cziferszky@uibk.ac.at](mailto:monika.cziferszky@uibk.ac.at)

## Abstract:

Platinum (II) based chemotherapeutics are a cornerstone in the treatment of many malignancies. However, their severe toxicity and dose-limiting side-effects have rooted efforts in the medicinal inorganic community to develop better drug candidates with higher selectivity for tumor tissues and less problematic side effects. In the current study, we developed a cytotoxic platinum (II) complex based on a Zeise's salt substructure containing the nonsteroidal anti-inflammatory drug (NSAID) acetylsalicylic acid (ASA) as a ligand. Since the original complex displayed high reactivity against sulfur-containing biomolecules, the structure was optimized regarding its stability. Amino acids L-alanine,  $\beta$ -alanine and L-histidine were used as biocompatible chelating ligands to achieve this aim. Differences in the coordination sphere caused pronounced changes in the stability profiles of the Zeise-type precursor complexes **1-3**. Of the tested systems, coordination with L-Ala through N in *trans* position to ethylene (N-*trans*) showed the most promising results and was employed to stabilize the previously published complex **5**. The stability profiles of all complexes were evaluated by capillary electrophoresis and the biological activity was investigated *in vitro* in various tumor cell lines. To investigate the effect of the NSAID ligand on the mode-of-action, inhibition of cyclooxygenase enzymes was also tested. Platinum (II) complex **4** containing both the ASA and the Ala ligand showed improved stability and higher cytotoxicity, outperforming both **5** and **1**, exhibiting a cytotoxic activity at 25  $\mu$ M comparable to the reference drug cisplatin.

## Keywords:

anticancer; Zeise's salt; amino acid ligand; cyclooxygenase; capillary electrophoresis; platinum; IRMPD; acetylsalicylic acid; metallodrug

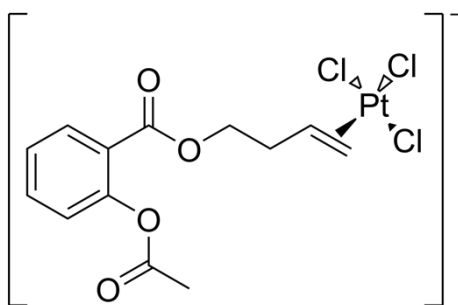
## Introduction

Cisplatin is the first and most widely used platinum-based anticancer drug for chemotherapy in standard health-care.<sup>1,2</sup> However, the use of this drug is limited by severe side effects, e.g. nephrotoxicity, hepatotoxicity, cardiotoxicity, nausea, vomiting, and ototoxicity.<sup>2,3</sup> Furthermore, various cancers show an intrinsic or acquired resistance to cisplatin and, due to the similar mechanism of action, exhibit cross-resistance against other platinum-based antitumor agents as well, i.e. oxaliplatin and carboplatin.<sup>4</sup> For these reasons, the motivation to improve the clinical performance of platinum-based chemotherapeutics leads to continuous research efforts to develop new drugs with higher efficacy, fewer side effects and with the capability to overcome intrinsic and acquired resistance.

A reasonable strategy to overcome the above-mentioned drawbacks is to consider a different therapeutic target, which also provides higher selectivity for tumor cells. Particularly interesting candidates are cyclooxygenases (COXs) and especially COX-2.<sup>5</sup> There are two isoforms for COXs, namely COX-1 and COX-2. The former is constitutively expressed in the tissues and its activity is related to normal physiological activity of cells. The latter, on the other hand, is an inducible form not detected in most tissues (except for kidney, seminal vessels and central nervous system) and is usually related to inflammatory response.<sup>5</sup> COXs are responsible for the biosynthesis of prostanoids. The first step in the synthetic pathway is the conversion of arachidonic acid to the highly unstable prostaglandin (PG) G<sub>2</sub>, which rapidly forms PGH<sub>2</sub>, and is subsequently converted by other enzymes into several PGs, the most abundant of which is PGE<sub>2</sub>.<sup>6</sup>

COX-2 is overexpressed in several tumors, including colorectal, breast, stomach, lung, and pancreatic cancer.<sup>7</sup> Moreover, there are suggestions that higher levels of COX-2 may be related to a bad prognosis for patients and that increased PG levels in cancer cells can also be caused by chemo- and radiotherapy.<sup>8</sup> Several studies highlight how COX-2 is likely involved in carcinogenesis and cancer progression, affecting aspects like xenobiotic metabolism, angiogenesis, inhibition of apoptosis, immunosuppression, and invasiveness.<sup>9</sup> Also, there is evidence for PGE<sub>2</sub> to contribute in angiogenesis, tumor promotion, and cellular apoptosis resistance.<sup>10</sup> The use of COX-2 selective inhibitors is often addressed as a powerful tool in the fight against cancer. A clear example is the COX-2 selective inhibitor celecoxib, which has demonstrated its efficacy against the familial adenomatous polyposis (FAP), a rare disease also studied for defining therapies against sporadic colorectal cancer. The efficacy of Celecoxib led to its approval by the FDA as adjunctive therapy for the treatment of FAP in the USA.<sup>11,12</sup> Another example is the COX-2 selective inhibitor rofecoxib, which was found to increase apoptosis and reduce proliferation in a Lewis lung (3LL) tumor cell line in a dose-dependent and time-dependent way.<sup>12</sup> Moreover, several pre-clinical studies suggest the possibility for COX-2 selective inhibitors to enhance the effects of chemo- and radiotherapy.<sup>8</sup> All these studies support the hypothesis that COX-2 selective inhibitors may be an interesting class of compounds as chemo-preventive, cytostatic or cytotoxic agents, given the well-known low side-effect profile compared to classic and non-selective NSAIDs.<sup>13</sup>

In our research group, one of the first discovered organometallic compounds, potassium trichloro(ethylene)platinate (II) or Zeise's salt (ZS), was investigated as a metal core for a possible new drug concept.<sup>14</sup> A promising compound was obtained by combining ZS with acetylsalicylic acid (ASA). In a series of ASA-modified Zeise-derivatives with different linker lengths, potassium {trichlorido[η<sup>2</sup>-(but-3-en-1-yl)-2-acetoxybenzoate]platinate(II)} (Pt-Butene-ASA, **5**) (Figure 1) exhibited high inhibition of COX-1, moderate inhibition of COX-2 and moderate activity against different tumor cell lines.<sup>4,14</sup>



5

Figure 1 Structure of potassium {trichlorido[ $\eta^2$ -(but-3-en-1-yl)-2-acetoxybenzoate]platinate(III)} (Pt-Butene-ASA, 5)

These inspiring results oriented the research of our group on the optimization of the lead-structure. A desirable feature is an increased selectivity for COX-2 inhibition, together with higher activity. We observed that, especially for the complexes with a propene-linker, the presence of water is detrimental for the stability of these substances.<sup>4,14</sup> Moreover, the reaction of complex **5** with sulfur containing biomolecules, e.g. ubiquitin or substance P, results in an immediate loss of the olefinic ligand. The main reason behind this degradation pathway relies on the strong *trans*-labilizing effect of the olefin, which causes the chlorido ligand in *trans* position to be easily exchanged by a suitable nucleophile. If the new donor also exhibits a strong *trans*-labilizing effect, like e.g. the sulfur of methionine, fast cleavage of the platinum-olefin bond is observed.<sup>15</sup> Considering the importance of solubility and stability in an aqueous environment for a drug candidate, the improvement of these parameters is essential and may also improve the cytotoxicity profile.

The degradation reaction of ZS in an aqueous environment is mediated by the exchange of the labile chlorido ligand *trans* to ethylene with a molecule of water.<sup>16,17</sup> The aquo ligand deprotonates and undergoes reductive elimination leading to insoluble platinum(0). A possible strategy to protect this point of weakness is to exchange the *trans*-ligand with a less labile one, like an amine. The use of polydentate ligands should further improve the stability of this kind of complex due to the chelating effect. Amino acids can be particularly suitable ligands for this purpose on account of their high biocompatibility, and for their hydrogen bond donor and acceptor groups, which may improve the water solubility. Moreover, they can be highly modulated by changing the side chain or the distance between the amino and carboxylic group.

Panunzi *et al.* reported the first synthesis for three Zeise-type complexes bearing an amino acid as chelating ligand in 1966. They chose glycine, racemic alanine and  $\beta$ -phenylalanine and obtained the respective products as “yellow, stable, non-ionic complexes corresponding to the general formula: chloro-ethylene-amino-acid-Platinum(II)”.<sup>18</sup> A few years later the configuration of the complex [Pt(C<sub>2</sub>H<sub>4</sub>)Cl(Gly)] was investigated and it was found to be the *N-trans* isomer, referring to the position of ethylene.<sup>19</sup> In 1970, the *ethylene,O-trans* isomer of the same complex was prepared to confirm the previous study.<sup>20</sup> The mechanism and kinetic of the formation of the (*ethylene,N-trans*)-[Pt(C<sub>2</sub>H<sub>4</sub>)(Ala)Cl] complex was investigated in depth using UV spectroscopy at a fixed pH range (3-4) and at variable concentrations of the alaninato ion, controlled by modulation of the pH.<sup>21</sup> In these investigations an acidic pH was chosen with two aims. On one hand the kinetics of the complex formation was slowed down, allowing the differences in the spectra to be detected for the available instruments. On the other hand, possible side-reactions of ZS were avoided by the low pH. About 10 years later, Erickson *et al.* discovered a thermodynamic preference for the *ethylene,O-trans* isomer over the corresponding *N-trans* isomer for [Pt(olefin)Cl(Gly)] complexes using NMR spectroscopy.<sup>22</sup> Also, this study was conducted in an acidic pH range (4-5) for the same reasons as mentioned above. Cavoli *et al.* succeeded in 1986 in obtaining the first crystal structure of the (*ethylene,N-trans*)-[Pt(C<sub>2</sub>H<sub>4</sub>)Cl( $\beta$ -Ala)] and, based on this and on the UV spectra, proposed the mechanism of formation of the complex as well as

the kinetics of the reaction.<sup>23</sup> An application of Zeise-type complexes with amino acid ligands in a biological or medical field has not been reported in the literature to date.

In the current study, we have synthesized Zeise's salt derivatives with L-alanine,  $\beta$ -alanine and L-histidine (complexes **1-3**, Figure 2) and investigated their stability and biological properties. The ethylene on the Zeise's salt-alanine derivative was also successfully exchanged with a butene-modified acetylsalicylic acid ligand (complex **4**, Figure 2). We investigated both, the effect of the chelating amino acid ligands on the stability profiles as well as the *in vitro* anticancer activity of the ZS derivatives on MCF-7 (breast cancer, COX positive), HT-29 (colon cancer, COX positive), MDA-MB-231 (breast cancer, COX positive), and A2780cis (ovarian cancer, COX negative, cisplatin-resistant) tumor cell lines. Also, the COXs inhibitory activity of the complexes was tested to establish more insight into the structure activity relationship.

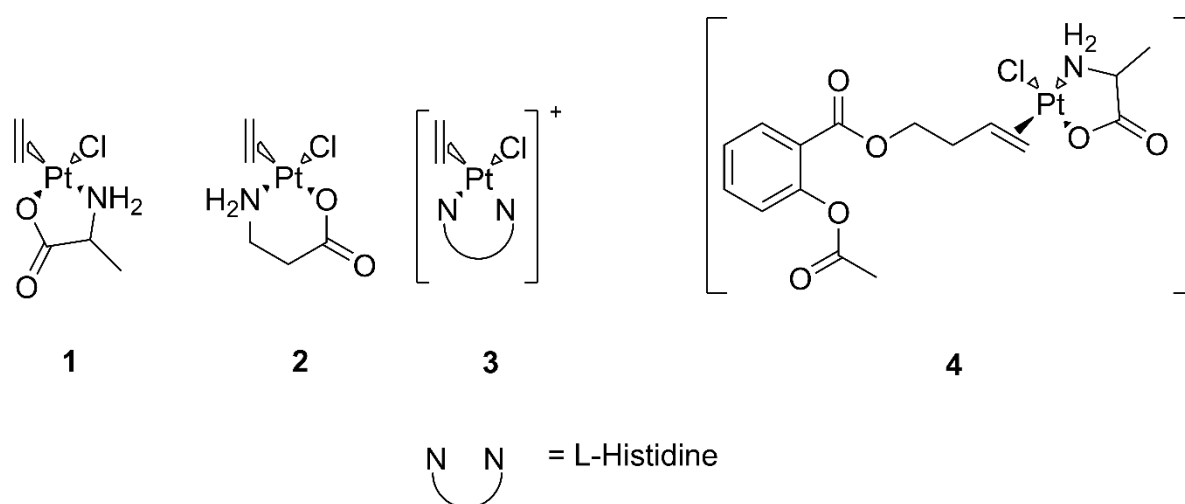


Figure 2 Structure of complexes **1-4** with three different coordination motifs of the amino acid ligands

## Experimental Section

### Materials

All chemicals were purchased either from Sigma-Aldrich, ABCR chemicals, Fluka, or Euriso-Top and were used as received. Solvents were purchased in appropriate purity and used as received. Water was deionized using a Millipore Milli-Q Gradient A10 Water Purification system (Merck Millipore, Billerica, MA, USA).  $^1\text{H}$ -,  $^{13}\text{C}$ -, and  $^{195}\text{Pt}$ - nuclear magnetic resonance (NMR) spectroscopy was performed on a Bruker Avance 4 Neo ( $^1\text{H}$  resonance frequency: 400 MHz). For the correct assignment of the signals,  $[\text{}^1\text{H}, \text{}^1\text{H}]$ -COSY,  $[\text{}^1\text{H}, \text{}^{13}\text{C}]$ -HSQC and  $[\text{}^1\text{H}, \text{}^{13}\text{C}]$ -HMBC 2DNMR experiments were carried out. Chemical shifts ( $\delta$ ) are given in parts per million (ppm). Coupling constants (J) are given in Hertz (Hz). Chemical shifts of  $^1\text{H}$ - and  $^{13}\text{C}$ -NMR experiments were referenced using the center of the internal residual peak of the solvent signal, which was related to tetramethylsilane (TMS) as  $\delta = 3.31$  ( $^1\text{H}$ -NMR) and  $\delta = 49.00$  ( $^{13}\text{C}$ -NMR) for  $\text{CD}_3\text{OD}$ ,  $\delta = 2.05$  ( $^1\text{H}$ -NMR) and  $\delta = 29.84$  ( $^{13}\text{C}$ -NMR) for  $(\text{CD}_3)_2\text{CO}$ , and  $\delta = 4.79$  ( $^1\text{H}$ -NMR) for  $\text{D}_2\text{O}$ <sup>24</sup>. High-resolution electrospray ionization mass spectrometry (HR-ESI-MS) was performed using an Orbitrap Elite mass spectrometer (Thermo Fisher Scientific, Waltham, MA, USA). IR spectra were recorded with a Bruker ALPHA FT-IR spectrometer, equipped with a Platinum-ATR module (diamond crystal) on a neat solid sample, if not stated differently. Capillary electrophoresis (CE) experiments were carried out on a 3D-CE system (Agilent, Santa Clara, CA, USA), which was equipped with an autosampler, a diode array detector (DAD) and a temperature-controlled capillary compartment. Agilent fused-silica capillaries (75  $\mu\text{m}$  inner diameter; 56 cm effective length, 64.5 cm total length) were purchased from VWR (Vienna, Austria). Purity determination and stability investigations were performed by CE experiments. All compounds are > 95% pure by CE (see Figure S22-S25).

## Synthesis

### (Ethylene,*N-trans*)(L-alaninato-N,O)chlorido( $\eta^2$ -ethene)platinate (II) (*N-trans*)[PtCl(L-Ala)(C<sub>2</sub>H<sub>4</sub>)] (**1**)

This complex was synthesized using the procedure reported by Fujita *et al.*<sup>20</sup>

*Yield:* 54 % as bright yellow crystals; *Purity:* 97.28 %; <sup>1</sup>H-NMR (400 MHz, CD<sub>3</sub>OD)  $\delta$  (ppm) 4.62 (s, 4H, CH<sub>2</sub>=CH<sub>2</sub>, <sup>2</sup>J<sub>H-Pt</sub> = 29.2 Hz), 3.78 (q, <sup>2</sup>J = 7.2 Hz, 1H, C $\alpha$ H), 1.46 (d, <sup>2</sup>J = 7.2 Hz, 3H, -CH<sub>3</sub>); <sup>13</sup>C-NMR (101 MHz, CD<sub>3</sub>OD)  $\delta$  (ppm) 188.8 (-COO), 76.6 (CH<sub>2</sub>=CH<sub>2</sub>), 54.9 (C $\alpha$ ), 19.4 (-CH<sub>3</sub>); <sup>195</sup>Pt-NMR (86 MHz, CD<sub>3</sub>OD)  $\delta$  (ppm) -2556. *Elemental Anal. Calcd* for C<sub>5</sub>H<sub>10</sub>ClNO<sub>2</sub>Pt: C, 17.32; H, 2.91; N, 4.04; Found: C, 17.26; H, 2.97; N, 3.68; *HR-MS:* [M + H]<sup>+</sup> exp 347.0116, calc 347.0121.

### (Ethylene,*O-trans*)( $\beta$ -alaninato-N,O)chlorido( $\eta^2$ -ethene)platinate (II) (*O-trans*)[PtCl( $\beta$ -Ala)(C<sub>2</sub>H<sub>4</sub>)] (**2**)

Complex **2** was obtained using a method similar to the one reported by Weninger *et al.*<sup>25</sup>

ZS (0.4 mmol, 1.0 eq) was dissolved in a vial in 1 mL of cold water.  $\beta$ -Alanine (0.4 mmol, 1.0 eq) was dissolved in 1 mL of cold water and added in one portion to the platinum solution under stirring. The mixture was cooled with an ice bath. After 15 min a solid precipitated, which was collected by filtration and washed several times with cold water, and then dried in vacuo to obtain the desired product.

*Yield:* 43 % as a pale-yellow powder; *Purity:* 96.00 % <sup>1</sup>H-NMR (400 MHz, CD<sub>3</sub>OD)  $\delta$  4.55 (s, 4H, CH<sub>2</sub>=CH<sub>2</sub>, <sup>2</sup>J<sub>H-Pt</sub> = 29.3 Hz), 3.19 (t, <sup>2</sup>J = 6.6 Hz, 2H, NH<sub>2</sub>-CH<sub>2</sub>-CH<sub>2</sub>, <sup>3</sup>J<sub>H-Pt</sub> = 16.10 Hz), 2.79 (t, <sup>2</sup>J = 6.6 Hz, 2H, CH<sub>2</sub>-CH<sub>2</sub>-COO); <sup>13</sup>C-NMR (101 MHz, CD<sub>3</sub>OD)  $\delta$  175.1 (-COO), 75.4 (CH<sub>2</sub>=CH<sub>2</sub>), 41.7 (NH<sub>2</sub>-CH<sub>2</sub>-CH<sub>2</sub>), 34.7 (CH<sub>2</sub>-CH<sub>2</sub>-COO); <sup>195</sup>Pt-NMR (86 MHz, CD<sub>3</sub>OD)  $\delta$  -3022. *Elemental Anal. Calcd* for C<sub>5</sub>H<sub>10</sub>ClNO<sub>2</sub>Pt + HCl: C, 15.67; H, 2.89; N, 3.66; Found: C, 15.59; H, 2.92; N, 3.62; *HR-MS:* [M + H]<sup>+</sup> exp 347.0120, calc 347.0121.

### (L-histidinato-N,N)chlorido( $\eta^2$ -ethene)platinate (II) [PtCl(His)(C<sub>2</sub>H<sub>4</sub>)] (**3**)

155 mg of ZS were dissolved in 0.75 mL of water in a vial protected from light. 62 mg of L-Histidine were suspended in 1 mL of water and added at 0°C. The suspension was allowed to stir at 0°C for 15 min. The reaction mixture was then filtered, washed 3 times with cold water, and air-dried.

*Yield:* 78 % as pale-yellow powder; *Purity:* 96.16 %; *NMR characterization was not possible due to low solubility of the complex; Elemental Anal. Calcd* for C<sub>8</sub>H<sub>12</sub>ClN<sub>3</sub>O<sub>2</sub>Pt + HCl: C, 21.34; H, 3.13; N, 9.33; Found: C, 21.43; H, 3.02; N, 9.47; *HR-MS:* [M]<sup>+</sup> exp 413.0341, calc 413.0339.

### (Ethylene,*N-trans*)(L-alaninato-N,O)chlorido( $\eta^2$ -(but-3-en-1-yl)-2-acetoxybenzoate)platinate (II) [PtCl(L-Ala)(ASA-Butene)] (**4**)

This complex was synthesized exchanging the ethylene on complex **1** with the olefin (but-3-en-1-yl)-2-acetoxybenzoate (ASA-Butene, **6**), following the procedure described by Weninger *et al.*<sup>4</sup>

*Yield:* 54% as beige solid; *Purity:* 97.00 %; <sup>1</sup>H NMR (400 MHz, (CD<sub>3</sub>)<sub>2</sub>CO)  $\delta$  8.05 (dd, <sup>3</sup>J = 7.8 Hz, <sup>4</sup>J = 1.8 Hz, 1H, ArH-6), 7.66 (ddd, <sup>3</sup>J = 7.8 Hz, <sup>3</sup>J = 8.1 Hz, <sup>4</sup>J = 1.8 Hz, 1H, ArH-4), 7.40 (ddd, <sup>3</sup>J = 7.8 Hz, <sup>3</sup>J = 7.8 Hz, <sup>4</sup>J = 1.2 Hz, 1H, ArH-5), 7.20 (dd, <sup>3</sup>J = 8.1 Hz, <sup>4</sup>J = 1.2 Hz, 1H, ArH-3), 6.24 (bd, J<sup>2</sup> = 39.8 Hz, 1H, N-H), 5.45 (bs, 1H, N-H), 5.38 – 5.24 (m, 1H, -CH=CH<sub>2</sub>), 4.74 – 4.55 (m, 2H, -OCH<sub>2</sub>-), 4.54 (dt, J<sup>3</sup> = 8.4, J<sup>2</sup> = 1.8 Hz, 1H, =CH $\alpha$ H $\beta$ ), 4.47 (dt, J<sup>3</sup> = 14.0, J<sup>2</sup> = 1.8 Hz, 1H, =CH $\alpha$ H $\beta$ ), 3.97 – 3.75 (m, 1H, C $\alpha$ H), 2.61 – 2.47 (m, 1H, -CH $\alpha$ H $\beta$ -), 2.30 (s, 3H, -OC(O)CH<sub>3</sub>), 2.28 – 2.17 (m, 1H, -CH $\alpha$ H $\beta$ -), 1.51 (d, J<sup>3</sup> = 7.1 Hz, 3H, -CH<sub>3</sub>); <sup>13</sup>C NMR (101 MHz, (CD<sub>3</sub>)<sub>2</sub>CO)  $\delta$  184.19 (d, J = 1.9 Hz, -CH-C(O)O-), 169.80 (-OC(O)CH<sub>3</sub>), 164.98 (-C(O)O-CH<sub>2</sub>-), 151.73 (C2), 134.82 (C4), 132.36 (C6), 126.89 (C5), 124.91 (C3), 124.51 (C1), 95.13 (d, J = 28.8 Hz, -CH=CH<sub>2</sub>), 72.97 (d, J = 10.0 Hz, -CH=CH<sub>2</sub>), 64.27 (-OCH<sub>2</sub>-), 54.43 (d, J = 11.0 Hz, C $\alpha$ ), 33.45 (d, J = 15.7 Hz, -CH<sub>2</sub>-CH=), 21.11 (-OC(O)CH<sub>3</sub>), 19.76 (d, J = 6.0 Hz, -CH<sub>3</sub>); <sup>195</sup>Pt NMR (86 MHz, (CD<sub>3</sub>)<sub>2</sub>CO)  $\delta$  -2536. *Elemental Anal. Calcd* for C<sub>16</sub>H<sub>20</sub>ClNO<sub>6</sub>Pt: C, 34.76; H, 3.65; N, 2.53; Found: C, 34.66; H, 3.82; N, 2.48; *HR-MS:* [M + H]<sup>+</sup> exp 553.0692, calc 533.0701.

## Stability

### Capillary electrophoresis

A solution of sodium tetraborate (final borate concentration of 50 mM) and sodium dodecyl sulfate (SDS; 100 mM) were used as background electrolyte (BGE). The pH of the BGE was adjusted to 9.3 by titration with 1 M NaOH. Every new capillary was rinsed with 1 M NaOH (45 min), water (45 min) and BGE (45 min), before the first use. The capillary was kept on a constant temperature of 25°C, whereas the sample carousel was temperature-controlled at 37°C. Sample injection was performed in hydrodynamic mode, applying a pressure of 50 mbar for 2 seconds on the inlet vial. The separation voltage was set at + 20 kV. If not stated differently, a wavelength of 195 nm was employed for the DAD detector. The analytic window was evaluated by using dodecaphenone as micellar marker and methanol (HPLC grade) as electroosmotic flow (EOF) marker. The run time required for the analysis was estimated to be 25 minutes. The capillary was flushed before every run with 0.1 M NaOH (3 min), water (3 min) and BGE (5 min). Every value is calculated from at least three independent measurements. The half-lives are presented as mean  $\pm$  standard deviation. All of the samples, buffers, and washing solutions were membrane filtered (0.22  $\mu\text{m}$  pore size). All samples employed for stability experiments were prepared using benzoic acid as internal standard (IS).

## Characterization

### IR multiple-photon dissociation (IRMPD) spectroscopy

Infrared multiple-photon dissociation (IRMPD) spectra were obtained at the Free Electron Laser for Infrared eXperiments (FELIX) facility (Nijmegen, The Netherlands) employing a commercial 3D quadrupole ion trap mass spectrometer (Bruker amaZon speed ETD) modified to permit for optical access to the trapped ions.<sup>26</sup> Samples were directly infused at a 120  $\mu\text{l h}^{-1}$  rate and ionized in positive ion mode using an electrospray ionization (ESI) source. The ions of interest were mass-selected and irradiated by a single IR pulse from the IR free electron laser. The FEL was operated at a 10 Hz repetition rate with a pulse energy of 40-100 mJ in the frequency range of 650-1900  $\text{cm}^{-1}$  with a step size of 5  $\text{cm}^{-1}$ . At each step, 6 replicate mass spectra were averaged. Spectra were recorded at several levels of laser pulse energy attenuation on order to prevent excessive depletion of the parent ions (saturation) and minimize the formation of fragment ions below the low mass cutoff of the MS.<sup>27</sup> To produce the IRMPD spectrum, the photofragmentation yield  $R$  ( $R = -\ln[I_p/(I_p + \Sigma I_f)]$ ), where  $I_p$  and  $I_f$  are the abundances of the parent ion and of a fragment ion, respectively) was plotted as a function of the wavenumber.<sup>28</sup> Finally, the yield was linearly corrected for the frequency-dependent variations in laser pulse energy.<sup>29</sup>

### Computational methods

Guess geometries were optimized using the DFT functional B3LYP-D3 and the 6-311++G(d,p) basis set for all atoms but platinum, for which the LanL2TZ basis set was employed.<sup>30</sup> Harmonic vibrational frequencies were computed at the same theory level to obtain IR spectra and thermodynamic corrections to the electronic energies. In addition, single-point energy calculations at the M06-2X/def2TZVP level were performed to evaluate the influence of a higher percentage of HF exchange on the relative energies of the isomers. B3LYP-D3 thermodynamic corrections were used to obtain relative enthalpies and Gibbs free energies at the M06-2X level. All DFT calculations were performed using Gaussian 09 rev. D.01.<sup>31</sup> To plot the calculated spectra, harmonic frequencies were scaled by 0.97 based on the good agreement with the IRMPD spectra.<sup>30,32</sup> Calculated linear IR spectra have been convoluted with a Gaussian profile of 20  $\text{cm}^{-1}$  (fwhm).

### X-ray crystallography

For single crystal structure analysis, crystals were measured into a stream of cold  $\text{N}_2$  (173 K) inside a Bruker D8 Quest diffractometer (Photon III C14). The instrument was equipped with an Incoatec Microfocus source generator (multi layered optics monochromatized Mo- $K_\alpha$  radiation,  $\lambda = 71.073$  pm). Multi-scan absorption corrections were applied with the program SADABS-2014/5. SHELXT and SHELXL program<sup>33,34</sup> were used for structure solution and refinement. Hydrogen atoms at ethylene were found and refined with isotropic

displacement parameters with bond restraints (95 pm). Additional details of the crystal structure investigation may be obtained from the Cambridge Crystallographic Data Centre (CCDC). The supplementary crystallographic data of **1a** and **1b** were deposited as CCDC number 2262096 and 2262097, respectively. These data are provided free of charge.

## Biological Testing

### Cell Lines

The ovarian carcinoma cell line A2780cis was kindly provided by the Department of Gynecology, Medical University Innsbruck.

The breast cancer cell line MCF-7 and the colon carcinoma cell line HT-29 were purchased from DSMZ, German Collection of Microorganisms and Cell Cultures, Braunschweig, Germany. The breast cancer cell line MDA-MB-231 was kindly provided by the Department of Hematology, Medical University Innsbruck.

The cell lines A2780cis and MDA-MB-231 were cultivated in RPMI 1640 without phenol red (PAN Biotech, Aidenbach, Germany), supplemented with L-glutamine (2 mM), 100 µg/mL penicillin and 100 µg/mL streptomycin, and FCS (10%) (all from Invitrogen Corporation, Gibco, Paisley, Scotland) at 37°C in a 5% CO<sub>2</sub>/95% air atmosphere and passaged twice per week. To maintain resistance, A2780cis cells were incubated every second week with Cisplatin (1 µM). The cell lines MCF-7 and HT-29 were grown in DMEM without phenol red (PAN Biotech, Aidenbach, Germany), containing L- glutamine and 100 µg/mL penicillin and 100 µg/mL streptomycin, sodium pyruvate (100 mM) (PAN Biotech) and FCS (10%) under the same conditions as the other cell lines.

### Analysis of cell growth inhibition

The exponentially growing cell lines were seeded at a density of 2000 cells/well for MCF-7 cells, 4000 cells/well for HT-29 cells and MDA-MB-231 cells and 8000 cells/well for A2780cis cells, respectively, into clear flat-bottom 96-well plates in triplicates. Following 24 h of incubation for adherent cell lines at 37°C in a humidified atmosphere (5% CO<sub>2</sub>/95% air), the compounds were added to reach the desired concentrations between 10 µM and 100 µM, respectively. All stock solutions were prepared in dimethylformamide (DMF) at a concentration of 100 mM and were then diluted with the respective cell-culture medium, to the appropriate concentrations. After another 72 h of incubation, the cellular metabolic activity was measured employing a 3-(4,5-dimethylthiazol-2-yl)-2,5-diphenyltetrazolium bromide (MTT) assay. Hereby, the yellow tetrazolium salt is converted to a purple formazan salt by functioning mitochondria. These purple crystals are then dissolved in DMSO and can be quantified via absorption measurements at 570 nm and 420 nm. The optical density of the particular medium was subtracted in order to exclude the unspecific staining caused by FCS-containing medium. The values were calculated with Excel 2019 (Microsoft, Redmond, WA, USA) using nonlinear regression and decal logarithm of the inhibitor versus variable slope equation, while the top constraint was set to 100%.

### Determination of COX-Inhibition

Inhibition of the isolated human recombinant COX-1 and COX-2 isoenzymes by the platinum complexes (10 µM and 25 µM) was evaluated using an enzyme immunoassay (EIA) (COX Inhibitor Screening Assay, Cayman Chemicals, Ann Arbor, Mi, USA) following the manufacturer's protocol. The incubation time of the compounds with the respective isoenzymes was exactly 2 min. The results are presented as the mean ± SD of three independent experiments, with two replicates of each experiment. The untreated control was set at 0% inhibition of COX activity.

## Results and discussion

### Synthesis and characterization

Complex **1** was synthesized using the procedure reported by Fujita et al.<sup>20</sup> and cubic bright-yellow crystals were obtained within hours. The amount of solvent, namely water, used for the reaction appears to be a critical factor for the isolation of the product, since complex **1** is moderately soluble in water. When a slightly lower concentration was used (0.4 mmol of platinum precursor instead of 0.5 mmol) keeping the amount of solvent constant, no crystallization occurred within a short time (3-4 hours). However, some colorless needle-shaped crystals formed after an extended period of time (5-6 weeks). The crystals obtained from both the conditions were analyzed *via* single crystal X-ray diffractometry.

The difference in concentration has led to the formation of two isomers. In particular, the *N-trans* isomer (**1a**, Figure 3) was obtained by complying with the procedure reported in the literature, while the *O-trans* isomer (**1b**, Figure 3) crystallized much slower from the solution with lower concentration. These results are also in agreement with the findings of Erickson *et al.*,<sup>22</sup> where the *N-trans* isomer was identified as the kinetic product and the *O-trans* isomer as the thermodynamic product of complexes of the type [PtCl(O ~ N)(olefin)].

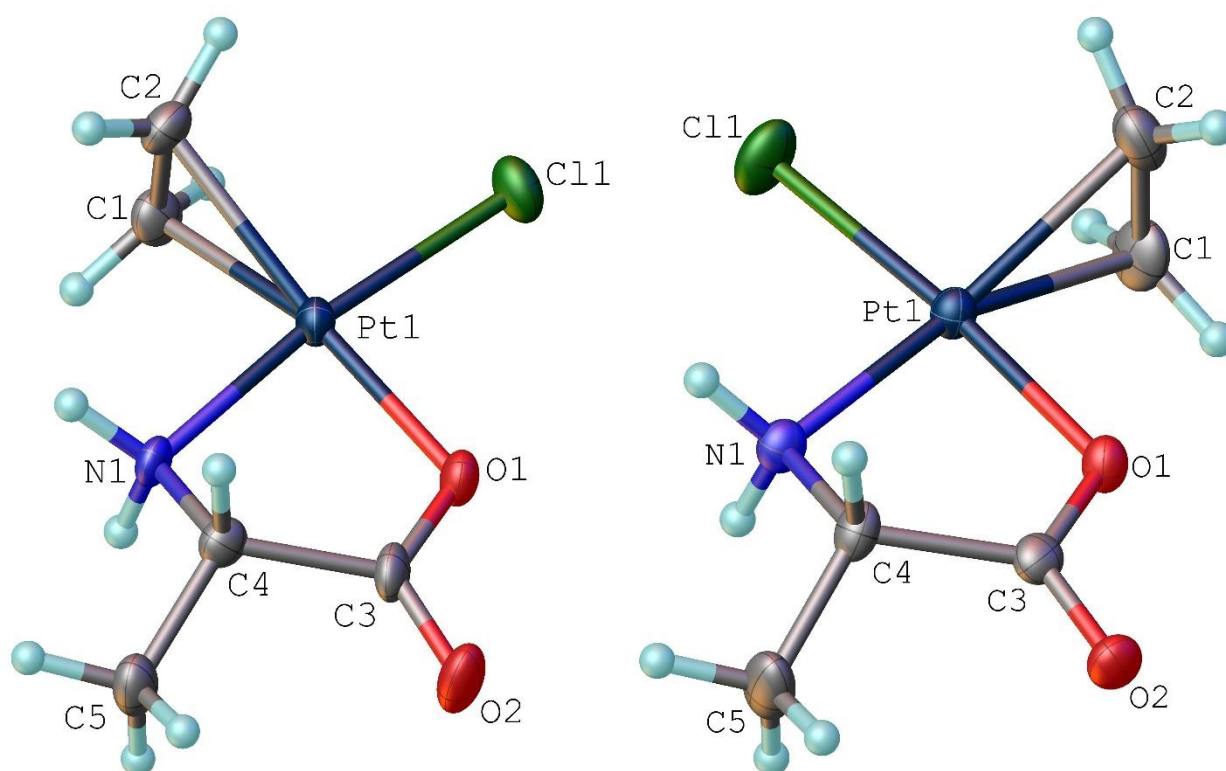


Figure 1 Oak Ridge Thermal-Ellipsoid Plot (ORTEP) of complexes **1a** (left) and **1b** (right)

Table 1 states the bond lengths and angles for the isomers **1a** and **1b**, in comparison to the structures of ZS and the *N-trans* isomer of complex **2** (**2a**), both reported in the literature:

Table 1 Comparison of the structural information of the two isomers of complex 1 (1a and 1b), ZS, and complex 2a.

	Complex	ZS <sup>35</sup>	1a	1b	2a <sup>23</sup>
Distances (Å)	C1=C2	1.37(3)	1.370(11)	1.382(7)	1.53(4)
	Pt-C1	2.121(19)	2.148(7)	2.125(7)	2.14(3)
	Pt-C2	2.134(19)	2.167(6)	2.136(7)	2.20(3)
	Pt-A (trans)	2.327(5)	2.054(5)	2.035(3)	2.09(2)
	Pt-A (cis)	2.314(7)	2.027(4)	2.037(4)	2.01(1)
	Pt-Cl	2.296(7)	2.2775(16)	2.3018(12)	2.277(8)
Angles (°)	Cl-Pt-A(trans)	90.2(3)	92.50(16)	92.10(9)	89.2(6)
	A(trans)-Pt-A(cis)	90.1(3)	82.44(19)	81.54(13)	92.1(7)

Both isomers **1a** and **1b** have a C=C bond length comparable to the one for ZS, meaning that the total effect of the  $\sigma$ -bonding and of the  $\pi$ -back bonding is not significantly affected. The platinum-carbon bond length is slightly increased for isomer **1a**, which suggests that the ethylene coordination to platinum is weaker. In comparison to complex **2a** the Pt-C distances are similar, but there is a higher C=C distance in the isomer with  $\beta$ -alanine, indicating a higher  $\pi$  back-donation. The distances of the nitrogen and the oxygen to the metal center highlight the stabilization induced by the chelating effect in all the derivatives. In fact, these distances are significantly shorter compared to the corresponding positions in ZS. Also, a significant distortion in the chelating angle of **1a** and **1b** was observed, it is about 10° narrower than the ideal value for a square planar geometry. This difference is related to the formation of a 5-membered ring in case of complex **1**. In fact, the corresponding chelating angle in **2a** is slightly above 90°, where the non-essential amino acid generates a 6-membered ring instead.

Table 2 lists the differences in chemical shifts (<sup>1</sup>H-, <sup>13</sup>C- and <sup>195</sup>Pt-NMR) for isomer **1a** in comparison to ZS and L-alanine. The protons of the ethylene in **1a** are de-shielded in comparison to the ones of ZS. This, together with the lower  $J_{Pt-H}$ , suggests a weaker coordination for ethylene, in agreement with the Pt-C distances (see Table 1). As expected, more or less every signal referring to the coordinated amino acid is shifted downfield, due to the  $\sigma$ -donation of the amino group and the  $\pi$ -donation of the carboxylate. The only exception are the protons of the methyl group, which remain unaffected. The <sup>195</sup>Pt-NMR spectrum shows that the metal ion is strongly de-shielded, compared to ZS.

Table 2 Comparison of the chemical shifts of the <sup>1</sup>H-, <sup>13</sup>C- and <sup>195</sup>Pt-NMR spectra of ZS, complex **1a**, complex **2**, L-alanine and  $\beta$ -alanine (all spectra recorded in CD<sub>3</sub>OD)

	ZS	1a	2	L-alanine	$\beta$ -alanine
C <sub>2</sub> H <sub>4</sub> [ppm]	4.39	4.62	4.55	N/A	N/A
<sup>2</sup> J <sub>H-Pt</sub> (C <sub>2</sub> H <sub>4</sub> ) [Hz]	32.6	29.2	29.3	N/A	N/A
C <sub><math>\alpha</math></sub> H [ppm]	N/A	3.78	N/A	3.58	N/A
-CH <sub>3</sub> [ppm]	N/A	1.46	N/A	1.46	N/A
-CH <sub>2</sub> -NH <sub>2</sub> [ppm]	N/A	N/A	3.19	N/A	3.07
-CH <sub>2</sub> -COO [ppm]	N/A	N/A	2.79	N/A	2.45
C <sub>2</sub> H <sub>4</sub> [ppm]	68.86	76.63	75.43	N/A	N/A
C <sub><math>\alpha</math></sub> H [ppm]	N/A	54.93	N/A	51.83	N/A
-CH <sub>3</sub> [ppm]	N/A	19.36	N/A	17.32	N/A
-CH <sub>2</sub> -NH <sub>2</sub> [ppm]	N/A	N/A	41.69	N/A	38.11
-CH <sub>2</sub> -COO [ppm]	N/A	N/A	34.66	N/A	34.32
-COO [ppm]	N/A	188.64	175.11	173.14	177.96
<sup>195</sup> Pt-NMR	-2769	-2557	-3032	N/A	N/A

Using the same reaction conditions as mentioned above, it was not possible to obtain complex **2**. Different strategies were tested (different bases, isolation of the potassium  $\beta$ -alaninate before the reaction with ZS),

but in all cases the solution turned brownish dark very quickly, indicating degradation of the precursor. However, an approach without the employment of a base was successful. Here, ZS and  $\beta$ -alanine were mixed in cold water and yielded the product as a bright yellow powder within 15 minutes. It was not possible to obtain crystals suitable for the analysis with the X-ray diffractometry, but the complex was fully investigated *via* NMR spectroscopy (see Table 2).

The protons of the ethylene in **2** are slightly downfield shifted compared to ZS, similar to complex **1a**, but to a lesser extent. The coupling constant between platinum and the olefinic protons in **2** is almost equal to the one of **1a**. However, in contrast to **1a**, the  $^{13}\text{C}$  signal of the carboxylate in **2** is more shielded than for the free  $\beta$ -alanine. Also, the platinum signal is shifted upfield in comparison to ZS.

Based on these findings, we conclude that the two complexes **1a** and **2** were obtained as different isomers. This highlights the critical role of the base on the selectivity of this reaction (see Figure 4). To confirm this hypothesis, we decided to follow the synthesis of complex **1** *via* NMR spectroscopy ( $^1\text{H}$ -,  $^{13}\text{C}$ - and  $^{195}\text{Pt}$ -, Figure S26, S27, and S28 respectively) with 1 eq. and without potassium bicarbonate. For this purpose, the reaction was set up with deuterium oxide as solvent. The results are summarized in Table 3:

Table 3 Comparison of the chemical shifts obtained from  $^1\text{H}$ -,  $^{13}\text{C}$ -, and  $^{195}\text{Pt}$ -NMR of L-Alanine, ZS, and complex **1** obtained with and without base (all spectra recorded using  $\text{D}_2\text{O}$  as solvent)

		$\text{C}_2\text{H}_4$	$\text{C}_\alpha\text{H}$	$-\text{CH}_3$	$-\text{COO}$	Pt
L-Ala	$^1\text{H}$ [ppm]	-	3.77	1.46	-	-
	$^{13}\text{C}$ [ppm]	-	50.39	16.09	175.72	-
ZS	$^1\text{H}$ [ppm]	4.66	-	-	-	-
	$^{13}\text{C}$ [ppm]	70.52	-	-	-	-
	$^{195}\text{Pt}$ [ppm]	-	-	-	-	-2796
<b>1b</b> w/o base	$^1\text{H}$ [ppm]	4.68	4.00	1.58	-	-
	$^{13}\text{C}$ [ppm]	71.05	49.83	15.88	174.33	-
	$^{195}\text{Pt}$ [ppm]	-	-	-	-	-2793
<b>1a</b> w base	$^1\text{H}$ [ppm]	4.77	4.00	1.52	-	-
	$^{13}\text{C}$ [ppm]	77.38	53.58	18.28	189.61	-
	$^{195}\text{Pt}$ [ppm]	-	-	-	-	-2535

The signals of the amino acid protons and carbons are shifted in both cases, confirming the coordination of the amino acid to platinum. The signals of the ethylene, carboxylate, and platinum are significantly shifted when a base is used and they correspond to the signals of the *N-trans* isomer **1a**. In the absence of base, the signals of the carboxylic carbon and of the platinum are both shifted to lower frequency, while they are shifted to higher frequency when base was used (Table 3). These evidences suggest that two different isomers **1a** and **1b** (Figure 3) were obtained, depending on the presence or absence of a base. This hypothesis is supported by the fact that the *O-trans* isomer **1b** was obtained, when a lower concentration of both the platinum precursor and the base were used (1:1), as the pH was lower in this case. Comparing these results with the chemical shifts as reported in Table 2, a similar trend for the isomer **1b** and complex **2** suggest that it was obtained as the *O-trans* isomer (**2b**).

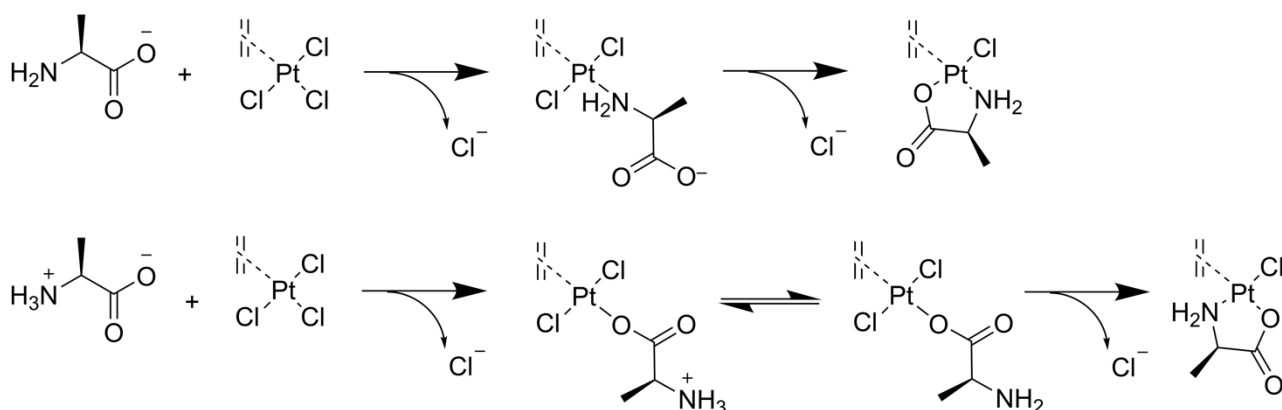


Figure 2 Proposed mechanism for the synthesis of the N-trans isomer **1a** (top) and the O-trans isomer **1b** (bottom).

The characterization and structure elucidation for complex **3** is strongly affected by its solubility. Despite trying an array of usual solvents, no solution with a suitable concentration for the characterization *via* NMR spectroscopy was obtained. The comparison of the IR spectra of complex **3** and of L-histidine (Figure 5) recorded from the neat solids proves that the amino acid is coordinated to the platinum core, as demonstrated by the shifts of the bands. In particular, two new bands at about 3450 cm<sup>-1</sup> and 1715 cm<sup>-1</sup> can be assigned to the O-H stretching and to the -C=O stretching of the carboxylic group respectively, indicating that the amino acid is not in the zwitterionic form. The complex band created by the stretching of the imidazole and side chain's C-H stretching is shifted from about 3000-3100 cm<sup>-1</sup> to about 3100-3200 cm<sup>-1</sup>, as consequence of the coordination. The band around 2800 cm<sup>-1</sup> in the histidine spectrum is also affected by the coordination to the platinum.

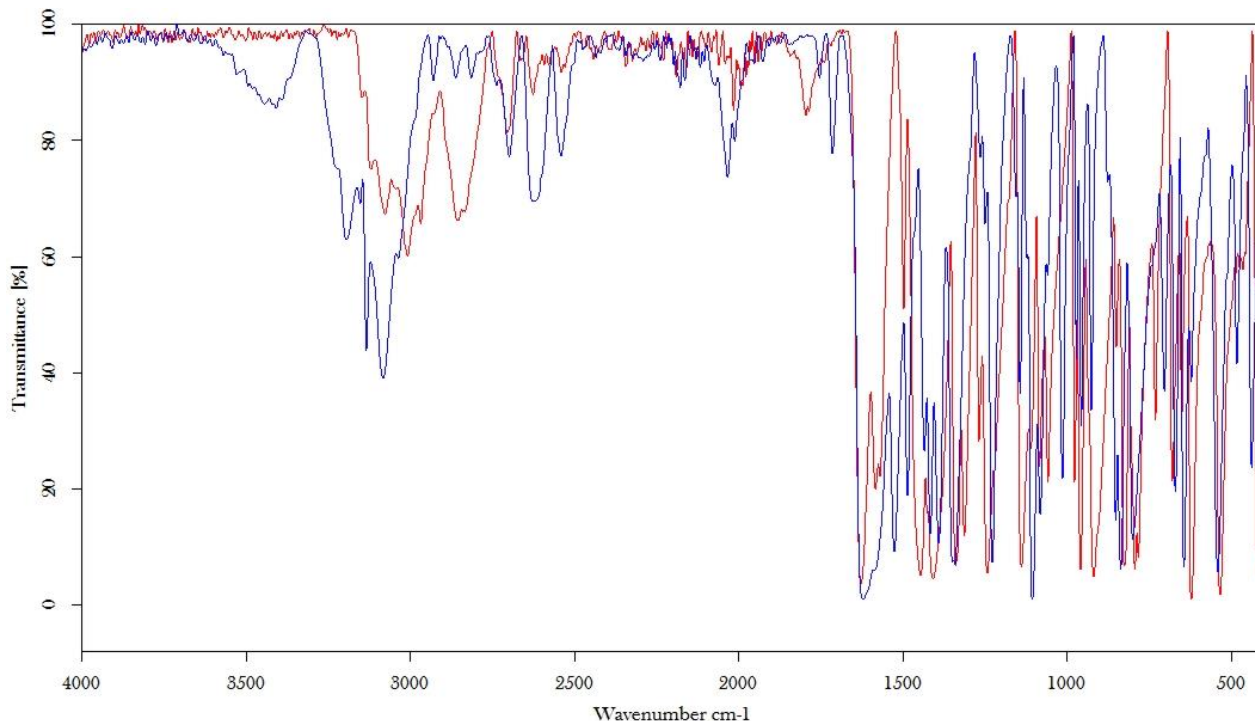


Figure 3 IR spectra of L-histidine (red) and complex **3** (blue) superimposed.

Further proof for the identity of complex **3** was obtained through HR-MS spectrum, where a characteristic cluster of signals at *m/z* 412-416 is visible and in agreement with the calculated isotopic distribution of complex **3** (see Figure S14).

In theory, histidine has four possible donor sites that can coordinate to platinum: the two N-atoms of the imidazole group ( $N_\pi$  and  $N_\tau$  being the closer and farther to the amino acidic chain, respectively), the carboxylic oxygen and the amino nitrogen ( $N_a$ ). However, binding of the metal to  $N_\tau$  does not allow the chelation of histidine to the metal due to steric constraints,<sup>30,36</sup> therefore three isomers presenting the  $N_\pi$  atom interacting with platinum, but differing for the other coordinating atoms were considered for further investigation. Figure 6 depicts the optimized structures of the three isomeric forms of complex **3** (**3\_1-3**). The two lowest energy structures show the amino nitrogen bound to platinum and are practically isoenergetic. They differentiate for the relative position of the ligand in the complex. In particular, **3\_1** shows the amino group of histidine bound to platinum in *trans* position to the ethylene ligand, vice versa **3\_2** presents the imidazole  $N_\pi$  atom in *trans* to  $C_2H_4$ . Isomer **3\_3** simulates the coordination of the histidine carboxylic group to platinum but the structure is significantly higher in energy, with a relative Gibbs free energy of 73.9 kJ/mol. To unequivocally assign the structure of complex **3** to a specific isomer, IRMPD spectroscopy was exploited.<sup>30,32,37,38</sup> Mass selected ions were submitted to IR photons of variable energy. Figure S15 shows the IRMPD spectrum together with the calculated spectra of isomers **3\_1-3**. The experimental bands are in good agreement with the calculated vibrational features of both **3\_1** and **3\_2**, allowing to attribute the structure of the sampled ions to either one of them or a combination of the two and to confirm that histidine coordinates through the  $N_\pi$  and  $N_a$  atoms to Pt(II). Additional details on the assignment of vibrational bands are reported in the SI in Table S1 and in the description of Figure S15.

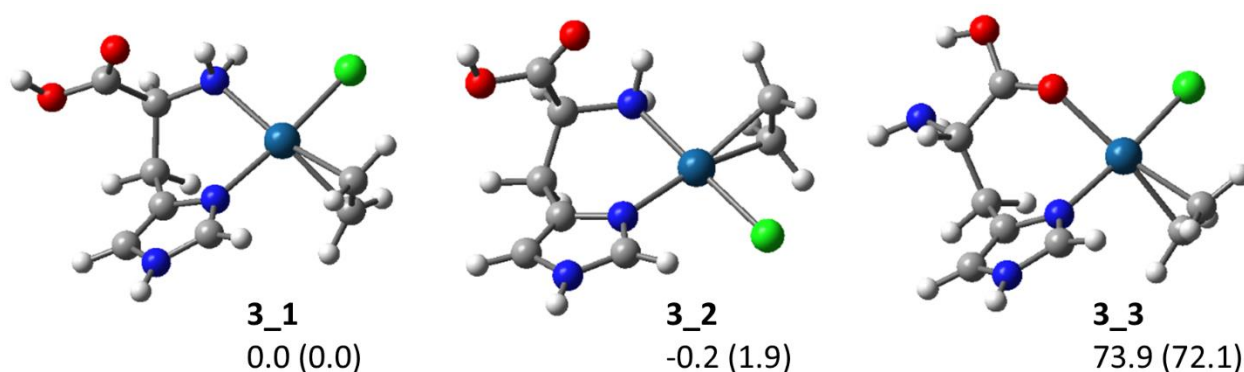


Figure 4 Optimized structures at the B3LYP level of isomers **3\_1-3** of complex **3**. Relative enthalpies (free energies) at 298 K calculated at the M06-2X level are reported in kJ mol<sup>-1</sup>. Both thermodynamic and spectroscopic evidences agree in indicating **3\_1** and **3\_2** as the only isomeric forms assayed.

Complex **4** was synthesized following the published procedure for complex **5**<sup>4</sup> and using complex **1a** as platinum precursor instead of ZS. NMR-spectroscopy reveals a single set of signals for the coordinated amino acid and only one peak in the <sup>195</sup>Pt-NMR, hence complex **4** was obtained as the *N-trans* isomer only. In general, the peaks of the olefinic protons of **4** are deshielded in comparison to the complex **5**, confirming the trend of the amino group in *trans* to destabilize the coordination of the olefin. Moreover, the electron density on the metal ion is lower in the case of complex **4**, as highlighted by the chemical shift towards lower field compared to complex **5**.

### Stability

The structure model<sup>39</sup> and the chemistry of Zeise's salt in aqueous solution<sup>17,40,41</sup> was investigated in depth in the past. The pronounced *trans* effect exerted by the ethylene causes the *trans*-chlorido ligand to be far more labile than the *cis*-chlorido ligand.<sup>41</sup> The kinetics of the exchange reaction of the *trans*-chlorido ligand with a water molecule is so fast, that Zeise's salt is converted to the *trans*-aquo complex quantitatively within 2 minutes of dissolution in water.<sup>40</sup> This intermediate is stable over weeks in acidic conditions, but undergoes quick reductive degradation in neutral or basic solutions.<sup>40</sup> The nature of the intermediates and products of this degradation pathways are still elusive.<sup>17</sup>

## Water

The stability of complexes **1-4** was tested in an aqueous solution, to investigate how the different ways of amino acid coordination impacts aqueous degradation. The stability of complex **5** was previously measured in a 50 % methanolic solution.<sup>4</sup> The half-life of this compound in the above-mentioned condition was found to be  $69.6 \pm 3.0$  h.

Table 4 Comparison of the half-life time ( $\tau_{1/2}$ ) determined in aqueous environment (with or without TMG) for complexes **1a**, **2b**, **3**, and **4**. (\*) These values are obtained from a 50% methanol solution.

	<b>1a</b>	<b>2b</b>	<b>3</b>	<b>4</b>
Water	> 72 h	$1.7 \pm 0.2$ h	N/A	> 72 h (*)
TMG	$24.3 \pm 2.6$ h	$0.77 \pm 0.08$ h	$12.0 \pm 3.0$ h	> 72 h

Complex **1a** is remarkably stable in water, with a half-life time higher than 72 h. No degradation products were detected at the electropherograms, which suggests precipitation of the complex or the degradation products.

Complex **2b**, however, showed a much lower stability ( $\tau_{1/2} = 1.7 \pm 0,2$  h), and fast conversion into another species with a higher effective mobility ( $-6.13 \times 10^{-5}$  cm<sup>2</sup>/sV vs  $-3.42 \times 10^{-4}$  cm<sup>2</sup>/sV for **2b**).

To better understand the nature of this intermediate, the reaction of complex **2b** with a large excess of water was followed by NMR spectroscopy (50 % D<sub>2</sub>O, Figure S31 and S32). The results highlight how the signal of the methylene in  $\alpha$ -position to the carboxylic group is the first to decrease. Simultaneously, a peak corresponding to the same methylene of the free amino acid is forming and increasing over time. A similar process is observed for the methylene in  $\alpha$ -position to the amino group, but the reaction is slower in this case. The signal of the ethylene ligand shows less changes in intensity and no overall loss of ethylene. Only two signals were detected in the <sup>195</sup>Pt-NMR experiments, probably for the intermediate and the final degradation product as shown in Figure 7. Based on the spectroscopic data, we conclude that the carboxylic group *trans* to the ethylene detached from the platinum in a first step, followed by the cleavage of the coordination bond between the amino group and the metal ion, forming the di-aquo complex.

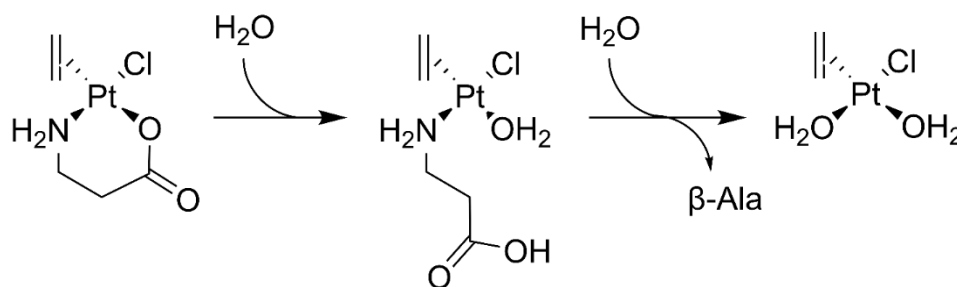


Figure 5 Proposed reaction of complex **2b** in an aqueous environment

Due to the solubility issues of complex **3**, it was not possible to obtain any information about the stability profile in purely aqueous conditions and a different approach was required (see below, TMG).

The stability profile of complex **4** is comparable to its precursor (complex **1a**). However, release of the olefin in aqueous environment was detected to an extent of about 20% after 72 h. The chelating amino acid enhances the stability of complex **4** (> 72 h) in comparison to compound **5** ( $69.6 \pm 3.0$  h). Also, complex **4** exhibited a better solubility in water.

## Trimethylglycine (TMG)

Kadokawa et al.<sup>42</sup> reported that a highly concentrated solution of trimethyl glycine (TMG, also known as betaine) is able to improve the solubility of cisplatin in water without affecting the pharmacological properties of this drug. The mechanism behind this effect seems to lie in the hydrogen bond acceptor property of the carboxylate of TMG, which establishes hydrogen bonds with the amino groups of cisplatin. Betaine is a non-toxic compound and is highly soluble in water. On the basis of this study, we decided to test the solubility of **3** in a highly concentrated (50% w/v) TMG aqueous solution. The platinum compound was soluble enough to allow the investigations with the established protocol for capillary electrophoresis. TMG has a strong absorption at low wavelengths and, therefore a wavelength of 230 nm was chosen instead of 195 nm for recording the electropherograms with TMG.

Complexes **1a**, **2b**, **3** and **4** were dissolved in 50% w/v TMG solution, diluted to a final TMG concentration of 25% and followed over time with the established CE protocol.

Complex **3** exhibited a half-life time of  $12.0 \pm 3.0$  h in these experimental conditions. A degradation product was detected at lower effective mobility ( $-4.19 \times 10^{-4}$  cm<sup>2</sup>/sV vs  $-2.90 \times 10^{-4}$  cm<sup>2</sup>/sV for **3**). The identification of this intermediate was not possible due to solubility issues. The stabilities of the other organometallic complexes follow the same trend as for the samples in aqueous solution ( $\tau_{1/2}$  (**1a**) =  $24.3 \pm 2.6$  h,  $\tau_{1/2}$  (**2b**) =  $0.77 \pm 0.08$  h,  $\tau_{1/2}$  (**4**) > 72 h).

In general, we observed that the stability is negatively affected by the use of TMG. A possible explanation for this phenomenon is that the 50 % TMG solution is slightly alkaline (pH =  $8,28 \pm 0,04$ ) and the basic environment can probably catalyze the degradation reaction of the Zeise-derivative complexes. The deprotonation of the amino groups involved in the coordination of the amino acids can also play a role.

To test whether TMG can coordinate to the platinum center, ZS was dissolved in a solution of TMG in deuterium oxide and <sup>195</sup>Pt-NMR spectra were recorded over-time (Figure S33). Based on these data, TMG does not interfere with the inner coordination sphere of ZS-derivatives.

## Biological tests

### Cytotoxic effects against cancer cell lines

In order to determine the antitumor activity of the platinum complexes, *in vitro* cytotoxicity tests were performed. Compounds **1-3** were tested with cisplatin as a reference on the breast cancer cell line MCF-7 and on the colon carcinoma cell line HT-29. Complexes **1**, **4**, and **5**, as well as the ligand (but-3-en-1-yl 2-acetoxybenzoate, **6**) were tested on MDA-MB-231 cells and A2780cis cells, also using cisplatin as reference. The metabolic activity as an indicator of cytotoxicity was determined by a classical 3-(4,5-Dimethylthiazol-2-yl)-2,5-diphenyltetrazoliumbromid (MTT) assay.

The amino acid derivatives of ZS **1-3** show almost no cytotoxicity. Compound **3** was slightly cytotoxic, with a metabolic activity of 70.74% at a concentration of 100  $\mu$ M on MCF-7 cells, whereas the other compounds displays a metabolic activity between 87.54% and 99.55% on the respective cell lines (Table S16).

To gain a preliminary insight into the required concentration to reduce the metabolic activity, compounds **1**, **4**, **5** and **6** were tested at 25  $\mu$ M. As seen in Figure 6, only the stability-optimized complex **4** was highly cytotoxic with a metabolic activity of 7.71 % similar to cisplatin (8.71 %). At A2780cis its activity is slightly weaker (33.13 % vs 4.71 %). The difference between the activity of complex **4** and compounds **1**, **5**, and **6** is statistically significant in both cell-lines. Noteworthy, the cytotoxic activity of complex **4** is statistically comparable to the one of cisplatin against both MDA-MB-231 and A2780cis cancer cells.

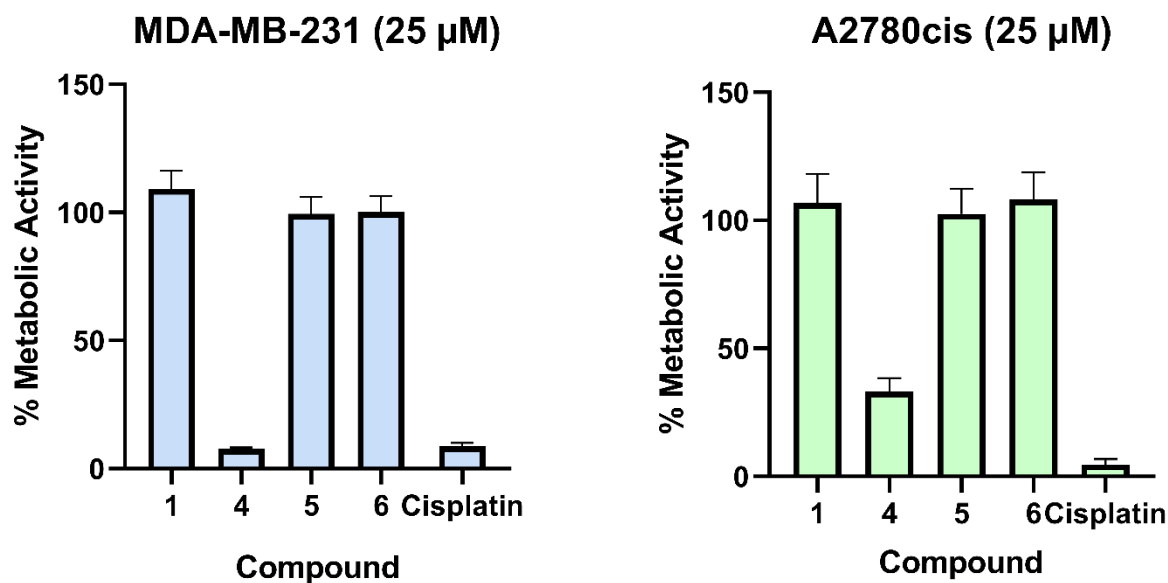


Figure 6: Metabolic activity of **1**, **4**, **5**, **6**, and cisplatin at 25 μM on MDA-MB-231 and A2780cis cells; mean of 5 independent experiments ± SEM

Therefore, concentration dependent cytotoxicity evaluations for compound **4** were performed (Figure 9). It showed a cytotoxic effect, bearing an IC<sub>50</sub> value of 15.41 ± 0.74 μM in MDA-MB-231 cells and 22.54 ± 0.97 μM in A2780cis cells. Accordingly, IC<sub>50</sub> values at MDA-MB-231 cell line of complex **4** and cisplatin were very similar (Table 5).

Table 5 IC<sub>50</sub> values calculated for complex **4** and the corresponding values of cisplatin (reference)

Compound	Metabolic activity IC <sub>50</sub> [μM]	
	MDA-MB-231	A2780cis
Cisplatin	13.27 ± 0.87	14.81 ± 1.23
<b>4</b>	15.41 ± 0.74	22.54 ± 0.97

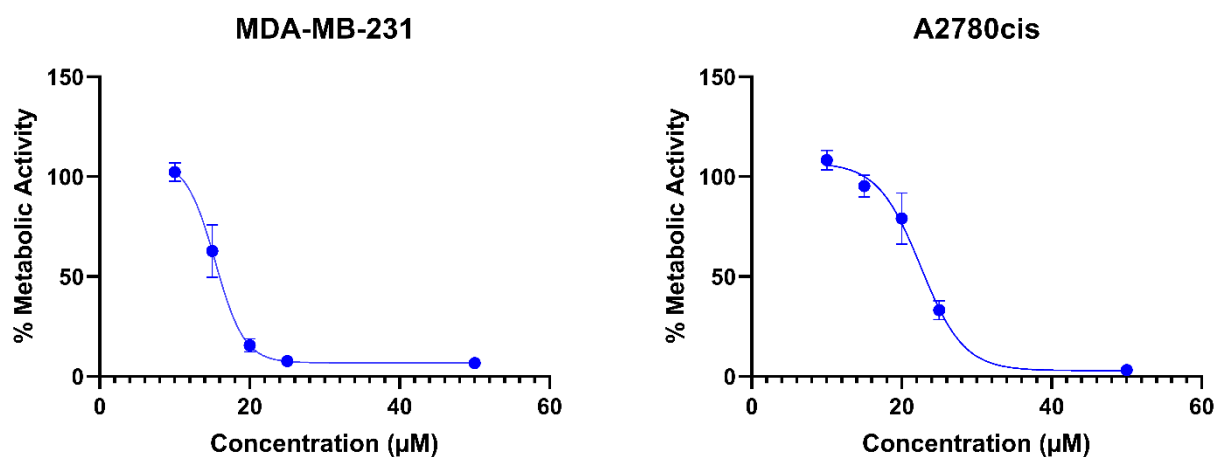


Figure 7: Metabolic activity profile of **4** on MDA-MB-231 and A2780cis cells; mean of 5 independent experiments ± SEM

The increased stability of complex **4** might play a role in its increased cytotoxicity compared to the precursor complex **5**. Also, compound **4** is neutral whereas **5** is negatively charged, which will likely impact cellular uptake of these platinum complexes.

### COX inhibition

Metal complexes containing an ASA moiety have been reported as inhibitor for COX-1/-2 previously.<sup>4,14,43–47</sup> Hence, an *in vitro* COX-1/-2 inhibition assay was performed to gain some insight into the mode of action of the platinum complex **4**. Hereby, the isolated enzymes were treated with a final concentration of 10  $\mu\text{M}$  and 25  $\mu\text{M}$  of substances **1**, **4**, **5** and **6**. Compounds **1**, **4** and **5** show a concentration dependent increase in both COX-1 and COX-2 inhibition (Figure S34).

Ligand **6** inhibits the COX isoenzymes to a low extent, which suggests that the platinum ion is important for the inhibition of the respective enzymes. All complexes **1**, **4** and **5** have a selectivity towards the inhibition of COX-1. However, compared to ZS, which is a selective COX-1 inhibitor (COX-1 inhibition at 10  $\mu\text{M}$  of 90.83%; COX-2 inhibition of 8.30%), and ASA (COX-1 inhibition at 10  $\mu\text{M}$  of 17.33%; COX-2 inhibition of 9.33%), a shift towards the inhibition of COX-2 can be observed (COX-2 inhibition at 10  $\mu\text{M}$  of 27.23%, 20.04% and 39.56% for **1**, **4** and **5**, respectively; Figure 8).

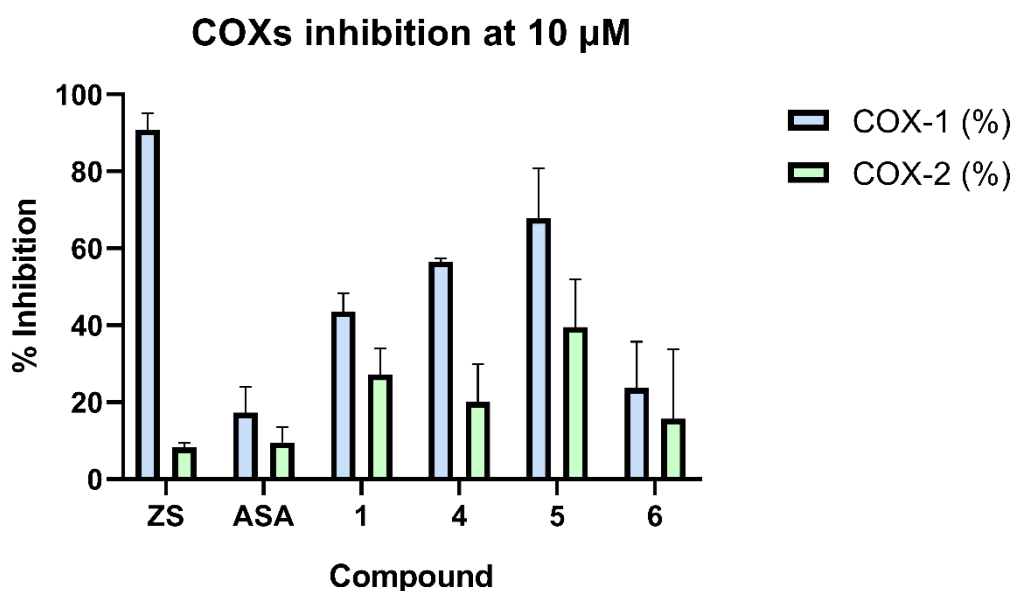


Figure 8: Inhibition of COX-1/-2 isoenzymes by Zeise's salt, ASA, **1**, **4**, **5** and **6** at 10  $\mu\text{M}$ ; mean of 3 independent experiments  $\pm$  SEM

The data obtained do not show any statistically relevant correlation between the cytotoxic activity and the COX-1 or COX-2 inhibition (Table S18). However, complex **4** shows improved efficacy against the COXs expressing MDA-MB-231 cell line, if compared to the A2780cis ovarian carcinoma cell line. These observations suggest that inhibition of COX-2 may play a role in the mode of action of complex **4**, but this enzyme does certainly not represent the exclusive target for this potential antitumor agent. Hence, we assume additional targets to be involved in the mode-of-action of compound **4**.

### Conclusion

This study addresses the stability issues known to affect platinum (II) complexes, and especially Zeise's salt derivatives. Amino acids were successfully employed as chelating agents to improve the aqueous stability as well as the cytotoxicity profile of a potential platinum (II) anticancer drug.

Three different amino acids resulting in different coordination motifs were chosen to investigate the influence on aqueous stability. Best results were achieved with L-alanine coordinating with the amino group in *trans* position to the ethylene forming a 5-membered ring with platinum, having a bite-angle of about 80°, as elucidated by the X-ray diffraction spectroscopy. The ethylene was then exchanged with an acetylsalicylic acid containing ligand to obtain the stability-optimized complex **4**. These structural changes also led to improved water solubility and enhanced cytotoxic activity in comparison to the previously published complex **5**. The comparison of the potency of complex **4** with the data obtained for complexes **1** and **5** highlights how both the olefinic and the amino acidic ligands are essential for the improved biological results. However, no significant improvement in the COXs inhibition was observed for complex **4**, compared to complex **5**. Moreover, complex **4** exhibits a better cytotoxic activity on both COX-2 positive and negative cancer cell lines. Its cytotoxicity on MDA-MB-231, in particular, was almost identical to that of cisplatin. However, the exact mechanism of action of this complex is still to be identified and will be subject of further investigations. We believe that complex **4** may be more resistant against nucleophilic attack to the platinum center from biological species, such as glutathione or other sulfur containing species. Investigations are planned to fully understand the potential behind this aspect.

**Supporting Information** NMR characterization spectra, electropherograms, crystal data and structure refinements, NMR experiments set up, IRMPD data and supplementary biological data (PDF)

**Author Contributions:** Conceptualization by A.C. and M.C.; funding acquisition and project administration by R.G.; Synthesis, characterization and stability profile determination of the complexes were performed by A.C.; M.C. recorded the MS spectra of the complexes; A.S. determined cytotoxicity values and evaluated the COX inhibition under the supervision of B.K.; K.W. recorded, processed, and analyzed the X-ray crystal structure of **1a** and **1b**; D.C., G.B., and J.O. performed the IRMPD spectroscopy measurements; D.C. performed the DFT calculations and analyzed the data obtained, comparing them with the experimental data from IRMPD spectroscopy experiments, under the supervision of M.E.C.; A.C., A.S., and D.C. wrote the original draft, M.C., B.K and M.E.C. reviewed and edited the manuscript. All authors made final corrections and have given approval to the final version of the manuscript.

**Acknowledgment** The authors would like to thank Roland Egger (Department of General, Inorganic and Theoretical Chemistry, University of Innsbruck) for performing the elemental analysis of the platinum complexes characterized in this study and Federico Ferro (Department of Pharmacy, University of Innsbruck) for support with the statistical analysis. The publication of this article (APC) has been funded by the University of Innsbruck. This research was funded by the Austrian Science Fund (FWF) [P-31166]. The research leading to these results has received funding from LASERLAB-EUROPE (grant agreement No. 871124, European Union's Horizon 2020 research and innovation programme). The authors gratefully acknowledge the Nederlandse Organisatie voor Wetenschappelijk Onderzoek (NWO) for the support experiments performed at the FELIX Laboratory.

# Current address: Sagl 26, A-6410 Telfs, Austria

- (1) Simpson, P. V.; Desai, N. M.; Casari, I.; Massi, M.; Falasca, M. Metal-Based Antitumor Compounds: Beyond Cisplatin. *Future Med. Chem.* **2019**, *11* (2), 119–135. <https://doi.org/10.4155/fmc-2018-0248>.
- (2) Alderden, R. A.; Hall, M. D.; Hambley, T. W. The Discovery and Development of Cisplatin. *J. Chem. Educ.* **2006**, *83* (5), 728–734. <https://doi.org/10.1021/ed083p728>.
- (3) Dasari, S.; Bernard Tchounwou, P. Cisplatin in Cancer Therapy: Molecular Mechanisms of Action. *Eur. J. Pharmacol.* **2014**, *740*, 364–378. <https://doi.org/10.1016/j.ejphar.2014.07.025>.
- (4) Weninger, A.; Baecker, D.; Obermoser, V.; Egger, D.; Wurst, K.; Gust, R. Synthesis and Biological

- Evaluation of Zeise's Salt Derivatives with Acetylsalicylic Acid Substructure. *Int. J. Mol. Sci.* **2018**, *19* (6), 1612. <https://doi.org/10.3390/ijms19061612>.
- (5) Ghosh, N.; Chaki, R.; Mandal, V.; Mandal, S. C. Cox-2 as a Target for Cancer Chemotherapy. *Pharmacol. Reports* **2010**, *62* (2), 233–244. [https://doi.org/10.1016/S1734-1140\(10\)70262-0](https://doi.org/10.1016/S1734-1140(10)70262-0).
  - (6) Rouzer, C. A.; Marnett, L. J. Cyclooxygenases: Structural and Functional Insights. *J. Lipid Res.* **2008**, *50* (Supplement), S29–S34. <https://doi.org/10.1194/jlr.r800042-jlr200>.
  - (7) Dannenberg, A. J.; Subbaramaiah, K. Targeting Cyclooxygenase-2 in Human Neoplasia: Rationale and Promise. *Cancer Cell* **2003**, *4* (6), 431–436. [https://doi.org/10.1016/S1535-6108\(03\)00310-6](https://doi.org/10.1016/S1535-6108(03)00310-6).
  - (8) Choy, H.; Milas, L. Enhancing Radiotherapy With Cyclooxygenase-2 Enzyme Inhibitors : A Rational Advance ? *JNCI J. Natl. Cancer Inst.* **2003**, *95* (19), 1440–1452. <https://doi.org/https://doi.org/10.1093/jnci/djg058>.
  - (9) Dannenberg, A. J.; Altorki, N. K.; Boyle, J. O.; Dang, C.; Howe, L. R.; Weksler, B. B.; Subbaramaiah, K. Cyclo-Oxygenase 2: A Pharmacological Target for the Prevention of Cancer. *Lancet Oncol.* **2001**, *2* (9), 544–551. [https://doi.org/10.1016/S1470-2045\(01\)00488-0](https://doi.org/10.1016/S1470-2045(01)00488-0).
  - (10) Zha, S.; Yegnasubramanian, V.; Nelson, W. G.; Isaacs, W. B.; De Marzo, A. M. Cyclooxygenases in Cancer: Progress and Perspective. *Cancer Lett.* **2004**, *215* (1), 1–20. <https://doi.org/10.1016/j.canlet.2004.06.014>.
  - (11) Steinbach, G.; Lynch, P. M.; Phillips, R. K. S.; Wallace, M. H.; Hawk, E.; Gordon, G. B.; Wakabayashi, N.; Saunders, B.; Shen, Y.; Fujimura, T.; Su, L.-K.; Levin, B.; Godio, L.; Patterson, S.; Rodriguez-Bigas, M. A.; Jester, S. L.; King, K. L.; Schumacher, M.; Abbruzzese, J.; DuBois, R. N.; Hittelman, W. N.; Zimmerman, S.; Sherman, J. W.; Kelloff, G. The Effect of Celecoxib, a Cyclooxygenase-2 Inhibitor, in Familial Adenomatous Polyposis. *N. Engl. J. Med.* **2000**, *342* (26), 1946–1952. <https://doi.org/10.1056/NEJM200006293422603>.
  - (12) Qadri, S. S. A.; Wang, J. H.; Redmond, K. C.; O'Donnell, A. F.; Aherne, T.; Redmond, H. P. The Role of COX-2 Inhibitors in Lung Cancer. *Ann. Thorac. Surg.* **2002**, *74* (5), 1648–1652. [https://doi.org/10.1016/S0003-4975\(02\)04022-5](https://doi.org/10.1016/S0003-4975(02)04022-5).
  - (13) Simon, L. S.; Weaver, A. L.; Graham, D. Y.; Kivitz, A. J.; Lipsky, P. E.; Hubbard, R. C.; Isakson, P. C.; Verburg, K. M.; Yu, S. S.; Zhao, W. W.; Geis, G. S. Anti-Inflammatory and Upper Gastrointestinal Effects of Celecoxib in Rheumatoid Arthritis. *JAMA* **1999**, *282* (20), 1921–1928. <https://doi.org/10.1001/jama.282.20.1921>.
  - (14) Meieranz, S.; Stefanopoulou, M.; Rubner, G.; Bendsdorf, K.; Kubutat, D.; Sheldrick, W. S.; Gust, R. The Biological Activity of Zeise's Salt and Its Derivatives. *Angew. Chemie - Int. Ed.* **2015**, *54* (9), 2834–2837. <https://doi.org/10.1002/anie.201410357>.
  - (15) Cziferszky, M.; Gust, R. Top-down Mass Spectrometry Reveals Multiple Interactions of an Acetylsalicylic Acid Bearing Zeise's Salt Derivative with Peptides. *JBIC J. Biol. Inorg. Chem.* **2020**, *25* (2), 285–293. <https://doi.org/10.1007/s00775-020-01760-9>.
  - (16) Allen, A. D.; Theophanides, T. Hydrolysis Constants of some Platinum(II) Chloro Complexes Containing Unsaturated Ligands. *Can. J. Chem.* **1965**, *43* (1), 290–295. <https://doi.org/10.1139/v65-032>.
  - (17) Joy, J. R.; Orchin, M. Hydrolyse des Zeise-Salzes. *Zeitschrift für Anorg. und Allg. Chemie* **1960**, *305* (3–4), 236–240. <https://doi.org/10.1002/zaac.19603050315>.
  - (18) Panunzi, A.; Palumbo, R.; Pedone, C.; Palaro, G. Monochloro-Amino-Acid-Olefin-Platinum(II) Complexes. *J. Organomet. Chem.* **1966**, *5* (6), 586–588. [https://doi.org/10.1016/S0022-328X\(00\)85167-0](https://doi.org/10.1016/S0022-328X(00)85167-0).

- (19) Kieft, J. A.; Nakamoto, K. The Synthesis and i.r. Spectrum of Chloro(Glycino)(Ethylene)Platinum(II). *J. Inorg. Nucl. Chem.* **1968**, *30* (11), 3103–3107. [https://doi.org/10.1016/0022-1902\(68\)80174-5](https://doi.org/10.1016/0022-1902(68)80174-5).
- (20) Fujita, J.; Konya, K.; Nakamoto, K. Platinum(II)-Olefin Complexes Containing Amino Acids. I. Preparation and Structure of Several Platinum(II)-Ethylene Complexes with Amino Acids. *Inorg. Chem.* **1970**, *9* (12), 2794–2796. <https://doi.org/10.1021/ic50094a038>.
- (21) Carturan, G.; Uguagliati, P.; Belluco, U. Mechanism of the Reaction of Zeise's Salt with DL- $\alpha$ -Alanine. *Inorg. Chem.* **1974**, *13* (3), 542–546. <https://doi.org/10.1021/ic50133a009>.
- (22) Erickson, L. E.; Brower, D. C. NMR Evidence for Thermodynamic Preference of Cis(N, Olefin) over Trans(N, Olefin) Isomers of Mixed Amino Acid-Olefin Complexes of Platinum(II). *Inorg. Chem.* **1982**, *21* (2), 838–840. <https://doi.org/10.1021/ic00132a076>.
- (23) Cavoli, P.; Graziani, R.; Casellato, U.; Uguagliati, P. Mechanism of Reaction of Zeise's Salt with  $\beta$ -Alanine. Crystal and Molecular Structure of Trans-(N,Olefin)[Pt(C<sub>2</sub>H<sub>4</sub>)( $\beta$ -Alaninato)Cl]. *Inorganica Chim. Acta* **1986**, *111* (2), L35–L37. [https://doi.org/10.1016/S0020-1693\(00\)84629-0](https://doi.org/10.1016/S0020-1693(00)84629-0).
- (24) Fulmer, G. R.; Miller, A. J. M.; Sherden, N. H.; Gottlieb, H. E.; Nudelman, A.; Stoltz, B. M.; Bercaw, J. E.; Goldberg, K. I. NMR Chemical Shifts of Trace Impurities: Common Laboratory Solvents, Organics, and Gases in Deuterated Solvents Relevant to the Organometallic Chemist. *Organometallics* **2010**, *29* (9), 2176–2179. <https://doi.org/10.1021/om100106e>.
- (25) Weninger, A. Novel Zeise-Type Complexes with Acetylsalicylic Acid Substructure: Design, Synthesis, Structural Analysis and Investigation of Their Cytotoxicity and Pharmacological Potential as COX Inhibitors Dissertation, Leopold-Franzens-Universität Innsbruck, **2019**.
- (26) Martens, J.; Berden, G.; Gebhardt, C. R.; Oomens, J. Infrared Ion Spectroscopy in a Modified Quadrupole Ion Trap Mass Spectrometer at the FELIX Free Electron Laser Laboratory. *Rev. Sci. Instrum.* **2016**, *87* (10), 103108. <https://doi.org/10.1063/1.4964703>.
- (27) Berden, G.; Derksen, M.; Houthuijs, K. J.; Martens, J.; Oomens, J. An Automatic Variable Laser Attenuator for IRMPD Spectroscopy and Analysis of Power-Dependence in Fragmentation Spectra. *Int. J. Mass Spectrom.* **2019**, *443*, 1–8. <https://doi.org/https://doi.org/10.1016/j.ijms.2019.05.013>.
- (28) Prell, J. S.; O'Brien, J. T.; Williams, E. R. IRPD Spectroscopy and Ensemble Measurements: Effects of Different Data Acquisition and Analysis Methods. *J. Am. Soc. Mass Spectrom.* **2010**, *21* (5), 800–809. <https://doi.org/10.1016/j.jasms.2010.01.010>.
- (29) van Geenen, F. A. M. G.; Kranenburg, R. F.; van Asten, A. C.; Martens, J.; Oomens, J.; Berden, G. Isomer-Specific Two-Color Double-Resonance IR2MS3 Ion Spectroscopy Using a Single Laser: Application in the Identification of Novel Psychoactive Substances. *Anal. Chem.* **2021**, *93* (4), 2687–2693. <https://doi.org/10.1021/acs.analchem.0c05042>.
- (30) Corinti, D.; De Petris, A.; Coletti, C.; Re, N.; Chiavarino, B.; Crestoni, M. E.; Fornarini, S. Cisplatin Primary Complex with L-Histidine Target Revealed by IR Multiple Photon Dissociation (IRMPD) Spectroscopy. *ChemPhysChem* **2017**, *18* (3), 318–325. <https://doi.org/https://doi.org/10.1002/cphc.201601172>.
- (31) Frisch, M. J.; Trucks, G. W.; Schlegel, H. B.; Scuseria, G. E.; Robb, M. A.; Cheeseman, J. R.; Scalmani, G.; Barone, V.; Mennucci, B.; Petersson, G. A.; Nakatsuji, H.; Caricato, M.; Li, X.; Hratchian, H. P.; Izmaylov, A. F.; Bloino, J.; Zheng, G.; Sonnenberg, J. L.; Hada, M.; Ehara, M.; Toyota, K.; Fukuda, R.; Hasegawa, J.; Ishida, M.; Nakajima, T.; Honda, Y.; Kitao, O.; Nakai, H.; Vreven, T.; Montgomery, J. A., Jr.; Peralta, J. E.; Ogliaro, F.; Bearpark, M.; Heyd, J. J.; Brothers, E.; Kudin, K. N.; Staroverov, V. N.; Keith, T.; Kobayashi, R.; Normand, J.; Raghavachari, K.; Rendell, A.; Burant, J. C.; Iyengar, S. S.; Tomasi, J.; Cossi, M.; Rega, N.; Millam, J. M.; Klene, M.; Knox, J. E.; Cross, J. B.; Bakken, V.; Adamo, C.; Jaramillo, J.; Gomperts, R.; Stratmann, R. E.; Yazyev, O.; Austin, A. J.; Cammi, R.; Pomelli, C.; Ochterski, J. W.; Martin,

R. L.; Morokuma, K.; Zakrzewski, V. G.; Voth, G. A.; Salvador, P.; Dannenberg, J. J.; Dapprich, S.; Daniels, A. D.; Farkas, Ö.; Foresman, J. B.; Ortiz, J. V.; Cioslowski, J.; Fox, D. J. Gaussian 09, Revision D.01, Gaussian, Inc.: Wallingford, CT, **2010**.

- (32) Paciotti, R.; Corinti, D.; Maitre, P.; Coletti, C.; Re, N.; Chiavarino, B.; Crestoni, M. E.; Fornarini, S. From Preassociation to Chelation: A Survey of Cisplatin Interaction with Methionine at Molecular Level by IR Ion Spectroscopy and Computations. *J. Am. Soc. Mass Spectrom.* **2021**, *32* (8), 2206–2217. <https://doi.org/10.1021/jasms.1c00152>.
- (33) Sheldrick, G. M. Crystal Structure Refinement with SHELXL. *Acta Crystallogr. Sect. C Struct. Chem.* **2015**, *71* (1), 3–8. <https://doi.org/10.1107/S2053229614024218>.
- (34) Sheldrick, G. M. SHELXT – Integrated Space-Group and Crystal-Structure Determination. *Acta Crystallogr. Sect. A Found. Adv.* **2015**, *71* (1), 3–8. <https://doi.org/10.1107/S2053273314026370>.
- (35) Jarvis, J. A. J.; Kilbourn, B. T.; Owston, P. G. A Re-Determination of the Crystal and Molecular Structure of Zeise's Salt,  $KPtCl_3 \cdot C_2H_4 \cdot H_2O$ . *Acta Crystallogr. Sect. B Struct. Crystallogr. Cryst. Chem.* **1971**, *27* (2), 366–372. <https://doi.org/10.1107/S0567740871002231>.
- (36) Appleton, T. G. Donor Atom Preferences in Complexes of Platinum and Palladium with Amino Acids and Related Molecules. *Coord. Chem. Rev.* **1997**, *166* (97), 313–359. [https://doi.org/10.1016/s0010-8545\(97\)00047-7](https://doi.org/10.1016/s0010-8545(97)00047-7).
- (37) He, C. C.; Kimutai, B.; Bao, X.; Hamlow, L.; Zhu, Y.; Strobehn, S. F.; Gao, J.; Berden, G.; Oomens, J.; Chow, C. S.; Rodgers, M. T. Evaluation of Hybrid Theoretical Approaches for Structural Determination of a Glycine-Linked Cisplatin Derivative via Infrared Multiple Photon Dissociation (IRMPD) Action Spectroscopy. *J. Phys. Chem. A* **2015**, *119* (44), 10980–10987. <https://doi.org/10.1021/acs.jpca.5b08181>.
- (38) He, C. C.; Hamlow, L. A.; Roy, H. A.; Devereaux, Z. J.; Hasan, M. A.; Israel, E.; Cunningham, N. A.; Martens, J.; Berden, G.; Oomens, J.; Rodgers, M. T. Structural Determination of Lysine-Linked Cisplatin Complexes via IRMPD Action Spectroscopy: NNs and NO– Binding Modes of Lysine to Platinum Coexist. *J. Phys. Chem. B* **2022**, *126* (45), 9246–9260. <https://doi.org/10.1021/acs.jpcc.2c06234>.
- (39) Chatt, J.; Duncanson, L. A. 586. Olefin Co-Ordination Compounds. Part III. Infra-Red Spectra and Structure: Attempted Preparation of Acetylene Complexes. *J. Chem. Soc.* **1953**, No. Part III, 2939. <https://doi.org/10.1039/jr9530002939>.
- (40) Leden, I.; Chatt, J. The Stability Constants of Some Platinous Halide Complexes. *J. Chem. Soc.* **1955**, No. 2936, 2936. <https://doi.org/10.1039/jr9550002936>.
- (41) Lokken, S. J.; Martin, D. S. Exchange and Substitution Reactions of Platinum(II) Complexes. IX. Trichloro-(Ethylene)-Platinate (II). *Inorg. Chem.* **1963**, *2* (3), 562–568. <https://doi.org/10.1021/ic50007a034>.
- (42) Kadokawa, R.; Fujie, T.; Sharma, G.; Ishibashi, K.; Ninomiya, K.; Takahashi, K.; Hirata, E.; Kuroda, K. High Loading of Trimethylglycine Promotes Aqueous Solubility of Poorly Water-Soluble Cisplatin. *Sci. Rep.* **2021**, *11* (1), 1–6. <https://doi.org/10.1038/s41598-021-89144-0>.
- (43) Ott, I.; Kircher, B.; Bagowski, C. P.; Vlecken, D. H. W.; Ott, E. B.; Will, J.; Bendsdorf, K.; Sheldrick, W. S.; Gust, R. Modulation of the Biological Properties of Aspirin by Formation of a Bioorganometallic Derivative. *Angew. Chemie - Int. Ed.* **2009**, *48* (6), 1160–1163. <https://doi.org/10.1002/anie.200803347>.
- (44) Rubner, G.; Bendsdorf, K.; Wellner, A.; Kircher, B.; Bergemann, S.; Ott, I.; Gust, R. Synthesis and Biological Activities of Transition Metal Complexes Based on Acetylsalicylic Acid as Neo-Anticancer Agents. *J. Med. Chem.* **2010**, *53* (19), 6889–6898. <https://doi.org/10.1021/jm101019j>.

- (45) Rubner, G.; Bendorf, K.; Wellner, A.; Bergemann, S.; Ott, I.; Gust, R. [Cyclopentadienyl]Metalcarbonyl Complexes of Acetylsalicylic Acid as Neo-Anticancer Agents. *Eur. J. Med. Chem.* **2010**, *45* (11), 5157–5163. <https://doi.org/10.1016/j.ejmech.2010.08.028>.
- (46) Zanellato, I.; Bonarrigo, I.; Ravera, M.; Gabano, E.; Gust, R.; Osella, D. The Hexacarbonyldicobalt Derivative of Aspirin Acts as a CO-Releasing NSAID on Malignant Mesothelioma Cells. *Metallomics* **2013**, *5* (12), 1604–1613. <https://doi.org/10.1039/c3mt00117b>.
- (47) Kowalski, K. Insight into the Biological Activity of Organometallic Acetylsalicylic Acid (Aspirin) Derivatives. *Chempluschem* **2019**, *84* (4), 403–415. <https://doi.org/10.1002/cplu.201900086>.